Mon. Not. R. Astron. Soc. **384,** 370–375 (2008) doi:10.1111/j.1365-2966.2007.12708.x

On the solar abundance of indium

N. Vitas,[1,2⋆] I. Vince,[2,3] M. Lugaro,[1,4] O. Andriyenko,[5,6] M. Gošić[2] and R. J. Rutten[1,7]

[1]*Sterrekundig Instituut, Utrecht University, PO Box 80000, 3508 TA Utrecht, the Netherlands*
[2]*Department of Astronomy, University of Belgrade, Studenstki trg 16, 11 000 Belgrade, Serbia*
[3]*Astronomical Observatory, Volgina 7, 11160 Belgrade, Serbia*
[4]*Centre for Stellar and Planetary Astrophysics, PO Box 28M Monash University, Victoria 3800, Australia*
[5]*ICAMER, NASU, 27 Akademika Zabolotnoho St., 03680 Kyiv, Ukraine*
[6]*Main Astronomical Observatory, NASU, 27 Akademika Zabolotnoho St., 03680 Kyiv, Ukraine*
[7]*Institutt for Teoretisk Astrofysikk, University of Oslo, PO Box 1029 Blindern, N-0315 Oslo, Norway*

Accepted 2007 November 12. Received 2007 November 8; in original form 2007 September 18

ABSTRACT

The generally adopted value for the solar abundance of indium is over six times higher than the meteoritic value. We address this discrepancy through numerical synthesis of the 451.13-nm line on which all indium abundance studies are based, both for the quiet Sun and the sunspot umbra spectrum, employing standard atmosphere models and accounting for hyperfine structure and Zeeman splitting in detail. The results, as well as a re-appraisal of indium nucleosynthesis, suggest that the solar indium abundance is close to the meteoritic value, and that some unidentified ion line causes the 451.13-nm feature in the quiet-Sun spectrum.

Key words: line: identification – nuclear reactions, nucleosynthesis, abundances – Sun: abundances.

1 INTRODUCTION

The solar abundance of indium is controversial because its generally accepted value significantly exceeds the meteoritic value. At a factor of 6 difference, this remains the largest unexplained discrepancy between meteoritic and solar abundance values. In this paper, we address this problem by considering the nucleosynthesis of indium and through indium line synthesis for the quiet solar photosphere and sunspot umbrae including hyperfine structure in detail.

The meteoritic indium abundance is $A_{\rm In}^{\rm m} = 0.80 \pm 0.03$ (Lodders 2003, and references therein) where $A_{\rm In} \equiv \log(n_{\rm In}/n_{\rm H}) + 12$ with $n_{\rm In}$ and $n_{\rm H}$ the indium and hydrogen particle densities, respectively. Table 1 summarizes the determinations of the solar indium abundance in the literature. All measurements are based on a single, very weak feature in the quiet-Sun spectrum at $\lambda = 451.1307$ nm which is commonly identified as one of the In I resonance lines. The initial result of Goldberg, Muller & Aller (1960) was based on an erroneous oscillator strength. The other three determinations scatter around $A_{\rm In}^{\odot} = 1.6$, the value listed in the compilation of Asplund, Grevesse & Sauval (2005). The 0.8 dex discrepancy with the meteoritic value cannot be explained by the usual uncertainties of abundance determination such as line strength measurement, imprecise atomic data and solar modelling deficiencies.

⋆E-mail: N.Vitas@astro.uu.nl

The origin of elements heavier than Fe is mostly attributed to neutron-capture processes (see Meyer 1994, for a review). *Slow* neutron capture (the *s* process) occurs for relatively low neutron densities ($\simeq 10^7$ cm^{-3}), while *rapid* neutron capture (the *r* process) occurs for relatively high neutron densities ($>10^{20}$ cm^{-3}). Allen (1978) analysed the Sn/In abundance ratio. He found that 'no combination of *r*- or *s*-process products even remotely resembling those which generally predict the Solar System abundances very successfully can give Sn/In as low as 1.4 arcmin (which results from taking $A_{\rm In}^{\odot} = 1.71$).

Recently, Gonzalez (2006b) suggested that because of its low condensation temperature (536 K, Lodders 2003), indium may have been depleted in chondritic meteorites to an abundance much smaller than the solar one. However, we note that, e.g. thallium has a similar condensation temperature (532 K, Lodders 2003) and a similar meteoritic abundance (0.78 ± 0.04) whereas its well-determined photospheric abundance (0.9 ± 0.2) is only slightly higher than the meteoritic one. In a sequel paper, Gonzalez (2006a) studied the indium abundance in a sample of 42 Sun-like stars of which five are known to host planets. He found a strong negative correlation between the [In/Fe] and [Fe/H] logarithmic abundance ratios. This trend is much steeper than the comparable relation for europium, which is a pure *r*-process element. However, one would expect a less steep trend for indium because it received contributions both from the *s* and the *r* processes.

In this paper, we once again scrutinize the solar indium abundance, paying specific attention to indium nucleosynthesis

Table 1. $A_{\rm In}^{\odot}$ determinations.

Authors	$A_{\rm In}^{\odot}$	Specified error
Goldberg et al. (1960)	1.16	
Lambert, Mallia & Warner (1969)	1.71	
Grevesse & Sauval (1998)	1.66	0.15
Bord & Cowley (2002)	1.56	0.20

(Section 2.1), indium line identification and appearance in the solar spectrum (Section 2.2), and indium line synthesis accounting for hyperfine structure both for quiet Sun and sunspot umbrae (Section 2.3). The conclusion is that, after all, the solar indium abundance is likely to be close to the meteoritic value.

2 ANALYSIS

2.1 Nucleosynthesis and the Sn/In ratio

In this section, we update the analysis of Allen (1978) considering the latest models for the origin of heavy elements. The indium and tin abundances in the Solar System are believed to have received contributions from both the *s* and the *r* processes, with roughly 30 and 60 per cent *s*-process production to In and Sn, respectively (e.g. Arlandini et al. 1999; Travaglio et al. 2004).

In Table 2, we present the Sn/In ratios associated to the most recent models of the *s* and the *r* processes. For the *s* process, we list different estimates of the ratio: two of them were derived using the classical approach for the *s* process, where abundances are calculated via a parametric model and another via the stellar model, where the building up of *s*-process abundances is modelled inside an asymptotic giant branch (AGB) stars (see Arlandini et al. 1999, for details). A further more realistic description of the Solar System distribution of abundance is given by models of the galactic chemical evolution (GCE), where yields from different generations of AGB stars are integrated in order to build up the Solar System abundances at the time and location of the formation of the Sun. In all descriptions, the Sn/In ratios remain very similar among the *s*-process estimates because during the *s* process, and far from nuclei with closed neutron shells, *s*-process abundances are determined by the $\sigma_{\rm A} N_{\rm A} \simeq$ constant rule, where $\sigma_{\rm A}$ is the neutron capture cross-section of isotope with atomic mass A, and $N_{\rm A}$ its abundance during the *s* process. The $\sigma_{\rm A}$ of In and Sn are determined with roughly 10 per cent uncertainties[1] and thus the Sn/In ratios from the *s* process have small nuclear uncertainties.

Table 2. Sn/In from different nucleosynthetic processes.

	Sn/In
s process (classical)[a]	39
s process (classical)[b]	46
s process (stellar)[a]	38
s process (GCE)[c]	34
r process (weak)[d]	32
r process (main)[d]	6
Solar value[e]	2.51
Meteoritic value[f]	20.42

[a]Arlandini et al. (1999), [b]Simmerer et al. (2004), [c]Travaglio et al. (2004), [d]Kratz et al. (2007), [e]Asplund et al. (2005), [f]Lodders (2003)

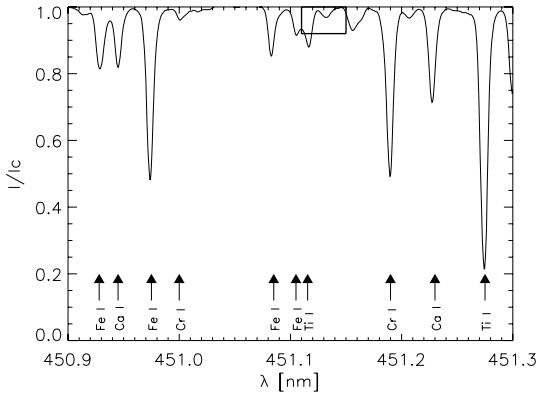

Figure 1. The spectral region around 451.13 nm in the Kitt Peak atlas of the quiet-Sun disc-centre photosphere. The intensity scale is normalized by the adjacent continuum value. The arrows specify line identifications copied from the Kitt Peak atlas.

For the *r* process, we take the recent parametric models of Kratz et al. (2007). Two *r*-process components, generated assuming different neutron densities, are introduced to build up the *r*-process abundances in the Solar System: the 'weak' *r* process produces elements up to tellurium and the 'main' *r* process produces elements from tellurium up to the actinides. The Sn/In ratio for the main *r*-process component is equal to six (Table 2), which confirms the estimate of Allen (1978) made using the simple argument that the *r* process would produce similar yields for close-by isotopes and that In and Sn have one and six stable isotopes that can be produced by the *r* process, respectively.

Finally, we note that recent *r*-process calculations indicate that the situation is likely to be much more complex, with several different components involved (Farouqi 2005). However, also in these more recent models no component with Sn/In < 8 is found (Kratz, personal communication).

2.2 Indium in the solar spectrum

The 451.13-nm line. The resonance line of In I at 451.13 nm ($5p^2P_{3/2} \rightarrow 6s^2S_{1/2}$) is the only indium line that has been identified in the solar spectrum. Fig. 1 shows this region in the disc-centre quiet-Sun Kitt Peak spectral atlas of Wallace, Hinkle & Livingston (1998). The small frame in Fig. 1 is enlarged in Fig. 2 and shows the region around 451.13 nm in detail. There are no significant differences with the Jungfraujoch atlas (Delbouille, Roland & Neven 1973). In the Kitt Peak atlas, the relatively strong feature at 451.1155 nm is attributed to Ti I, but this identification does not agree with Kurucz & Bell (1995) whose table instead suggests a line of Cr I at 451.1134 nm.

Other lines that may be expected in this narrow region are listed in Table 3 and indicated in Fig. 2. The lines of Ru I and Sc II are fully blended by the wing of the line at $\lambda = 451.1155$ nm. The four Fe II lines have high excitation energy (>10 eV) and low oscillator strengths; hence, they should not be present in the quiet-Sun spectrum. There are three candidate blends of the In line due to Sc I, V I and Sm I. All three belong to elements with a large nuclear spin, so that hyperfine splitting must be taken into account. Scandium and vanadium have only one stable isotope with $I = 7/2$. Samarium

[1] http://nuclear-astrophysics.fzk.de/kadonis/.

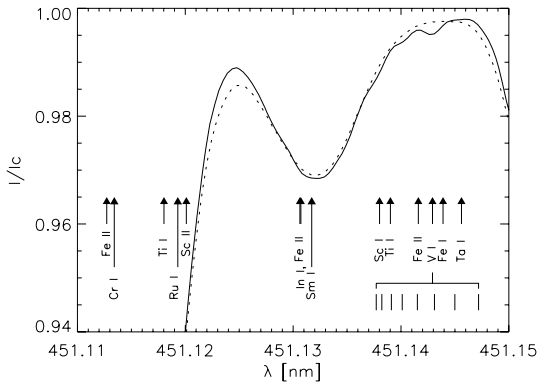

Figure 2. Enlargement of the frame in Fig. 1. Solid line: Kitt Peak atlas. Dotted line: Jungfraujoch atlas. The candidate lines of Table 3 are indicated by arrows. Positions of hyperfine components of the V I line are also indicated.

Table 3. Possible blends of In I 451.13 nm. The data are from Kurucz & Bell (1995) (K&B) and Kupka et al. (1999) (VALD).

Element	λ (nm)	E_l (eV)	log (*gf*)	Reference
Fe II	451.1127	11.31	−2.811	K&B
Cr I	451.1134	3.17	−2.366	K&B
Ti I	451.1170	0.50	−3.300	VALD
Ru I	451.1193	1.69	−1.070	K&B
Sc II	451.1201	7.87	−1.694	K&B
Fe II	451.1306	10.60	−3.338	K&B
In I	451.1307	0.27	−0.213	K&B
Sm I	451.1317	0.50	−0.013	K&B
Sc I	451.1380	1.85	−1.193	K&B
Ti I	451.1390	3.29	−4.076	VALD
Fe II	451.1416	11.29	−2.063	K&B
V I	451.1429	2.13	−1.520	K&B
Fe II	451.1439	10.72	−3.405	K&B
Ta I	451.1456	0.70	−1.730	K&B

has seven stable isotopes, two (^{147}Sm and ^{149}Sm) having non-zero nuclear spin $I = 7/2$. Unfortunately, data on hyperfine splitting are only available for the V I line (Kurucz & Bell 1995). The ground level of Sm I is split in seven sublevels, giving numerous weak transitions as indicated in Fig. 2. The Sm I 451.1317-nm line, attributed to Sm II by Gonzalez (2006a), is one of them. The In I line is not affected by the Ta I 451.1456-nm line as it is sufficiently far away.

The umbral spectrum in the Kitt Peak Sunspot Atlas of Wallace, Hinkle & Livingston (2000) shows a much stronger line at λ = 451.13 nm as illustrated in Fig. 3. Its core is clearly split in two strong components, with the red peak slightly stronger than the blue one. Gonzalez (2006a) attributes them to Zeeman splitting of the In I line. The upper solid curve in Fig. 3 represents the photospheric spectrum as a reference. The dotted curve is the observed umbral spectrum with sizable correction for straylight following Zwaan (1965), setting its amount to 60 per cent (i.e. the observed spectrum contains 60 per cent photospheric and 40 per cent umbral light). The choice of this value is discussed below. The broad triple-peaked feature to the right-hand side of the indium line is likely due to the hyperfine splitting of the V I line indicated in Fig. 2.

Other indium lines. Table 4 lists the other candidate lines of neutral and singly ionized indium. The other component of resonance multiplet (1) is $5p^2P_{1/2} \rightarrow 6s^2S_{1/2}$ at λ = 410.1765 nm. It is

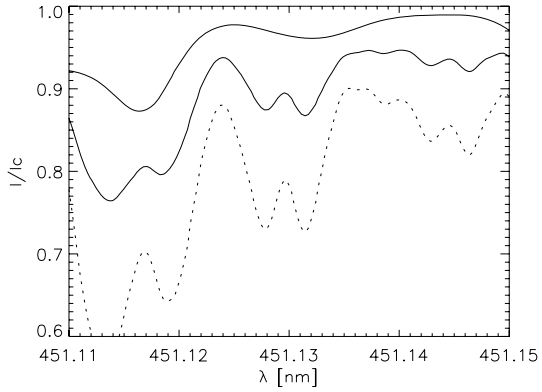

Figure 3. The spectral region around the 451.13-nm line in the Kitt Peak sunspot atlas. Lower solid curve: sunspot spectrum. Dotted curve: after subtraction of 60 per cent straylight. Upper solid curve: Kitt Peak quiet-Sun atlas for comparison. Each atlas profile is normalized to its own adjacent continuum.

located close to the centre of the Balmer Hδ line and is not recognizable in the quiet-Sun Kitt Peak atlas. The other indium lines are absent or completely blended or located in spectral regions that are not covered by the present solar atlases.

Since indium is mostly ionized (over 99 per cent throughout the photosphere assuming the Saha distribution), one would expect that the In II resonance line at 158.6 nm should be the strongest in the solar spectrum, but also this line is not clearly present in the atlas of Curdt et al. (2001).

2.3 Synthesis of the solar In I 451.13-nm line

Model atom. Oscillator strengths for the indium transitions were taken from Kurucz & Bell (1995) except for the 451.13-nm line for which Table 5 lists various values from the literature. We adopted the value of Fuhr & Wiese (2006). The indium hyperfine structure must be taken into account because the nuclear spin of In is $I = 9/2$. Values of the magnetic dipole (A) and electric quadrupole (B) constants of the hyperfine interaction for the lower and the upper levels of the In I multiplet 1 were taken from Jackson (1981) and Zaal et al. (1978).

The level splitting was evaluated from

$$\Delta E_F = \frac{C}{2}A + \frac{3C(C+1) - 4I(I+1)J(J+1)}{8I(2I-1)J(J-1)}B,$$

where $C = F(F+1) - J(J+1) - I(I+1), F = J+I, J+I-1, \ldots, |J-I|$ and J is the electronic angular momentum (e.g. Sobelman 1992). For the upper level with $J = 1/2$ only the first term in the Hamiltonian of the hyperfine interaction is present and is split into two sublevels ($F = 4, 5$), while the upper level is split into four sublevels ($F = 3, 4, 5, 6$). Hence, the selection rule ($\Delta F = -1, 0, 1$) implies that six hyperfine components are expected in the 451.13-nm transition. Relative intensities of these components were calculated from Wigner 6j coefficients assuming analogy with Russell–Saunders coupling (cf. Sobelman 1992). Table 6 specifies the resulting hyperfine structure components. Indium has two stable isotopes, but since the ratio of their abundances is ^{115}In:^{113}In = 95.7:4.3, the second isotope can be neglected.

Quiet-Sun profile synthesis. The radiative transfer code MULTI 2.2 of Carlsson (1992) was used for detailed synthesis of the In I 451.13-nm line profile.

Table 4. Candidate lines of In I and In II and their appearance in the Kitt Peak atlas (K, Wallace et al. 1998) and the atlas of Curdt et al. (2001; S). The wavelengths and oscillator strengths are from CD-ROM No. 23 of (Kurucz & Bell 1995).

Ionization stage	λ (nm)	log (*g f*)	E_l (eV)	Atlas	Comment
I	303.9357	−0.143	0.000	K	In the wing of Fe I 303.9321 nm
I	325.6087	0.170	0.274	K	In the wing of a strong line at λ = 325.613 nm
I	325.8559	−0.620	0.274	K	Between two strong lines
I	410.1765	−0.550	0.000	K	In the core of Hδ
I	451.1307	−0.213	0.274	K	The only identified line of In I
I	684.7440	−1.200	3.022	K	No line
I	690.0132	−1.510	3.022	K	Strong telluric line
II	78.3892	−3.092	0.000	S	No line
II	91.0951	−1.777	0.000	S	No line
II	92.7324	−3.170	0.000	S	Heavily blended
II	158.6450	0.393	0.000	S	Very weak unidentified line

Table 5. Values of log (*g f*) for In I 451.13 nm transition.

log (*g f*)	*A* (10^8 s^{-1})	Source
−0.308	0.806	L
−0.265	0.890	M
−0.213	1.003	K&B
−0.206	1.019	F&W
−0.167	1.115	C&B
−0.360	0.715	G&K W
−0.590	0.421	G&K D

L = Lambert et al. (1969), M = Morton (2000), K&B = Kurucz & Bell (1995), F&W = Fuhr & Wiese (2006), C&B = Corliss & Bozman (1962), G&K = Gurtovenko & Kostyk (1989) (W = value determined from the equivalent width, D = from the line depth).

Table 6. Hyperfine components of In I 451.13 nm with *r* the intensity of the component relative to the strongest one and Δλ the wavelength shift from the centre of gravity.

F_l	F_u	*r*	Δλ (pm)
5	4	33.84	3.14
4	4	50.76	2.38
3	4	53.84	1.93
6	5	100.00	−1.38
5	5	50.76	−2.58
4	5	18.46	−3.34

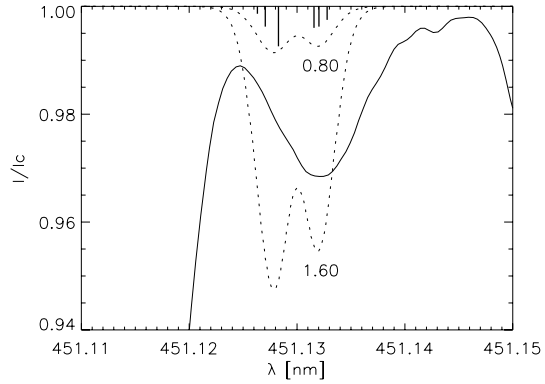

Figure 4. Synthetic profiles (dotted line) of the In I 451.13-nm line for $A_{\rm In}^{\odot}$ = 0.80 and 1.60 compared with the Kitt Peak atlas (solid line). The vertical bars at the top specify the wavelengths and relative intensities of the hyperfine components. They produce double peaks in the synthetic profiles.

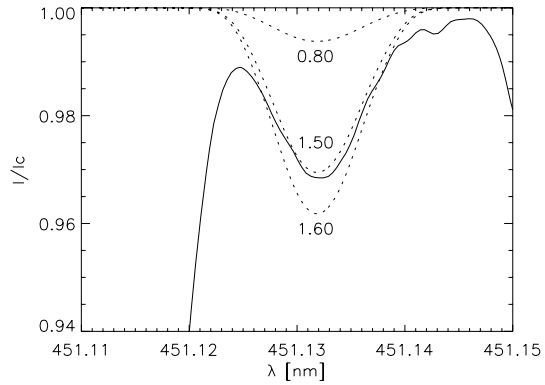

Figure 5. Synthetic profiles (dotted line) of the In I 451.13-nm line compared with the Kitt Peak atlas (solid line) after ad hoc convolution and wavelength shift.

As commonly done in solar abundance analysis (see Rutten 2002), we assume local thermodynamical equilibrium (LTE) and the model of Holweger & Müller (1974; henceforth HOLMUL) for the solar photosphere, including its microturbulence stratification. For the oscillator strength of In I 451.13 nm, we take the value of Fuhr & Wiese (2006). We computed line profiles both for the meteoritic abundance value $A_{\rm In}^{\rm m}$ = 0.80 and for the solar value $A_{\rm In}^{\odot}$ = 1.60 listed by Asplund et al. (2005). The resulting profiles are compared with the observed quiet-Sun profile in Fig. 4. The vertical bars specify the hyperfine structure components. It is obvious that neither computation fits the observed feature at all.

Fig. 5 illustrates the steps that are required to force a better match. The synthesized line was convoluted with a broad Gaussian profile with full width at half-maximum (FWHM) = 1.58 pm (1 pm = 10^{-3} nm), much wider than the instrumental broadening of the Fourier Transform Spectrometer (FTS) at Kitt Peak, and it was shifted redwards over Δλ = 2.35 pm. With these ad hoc measures a reasonable fit is obtained for indium abundance $A_{\rm In}^{\odot}$ = 1.50 (Fig. 5)

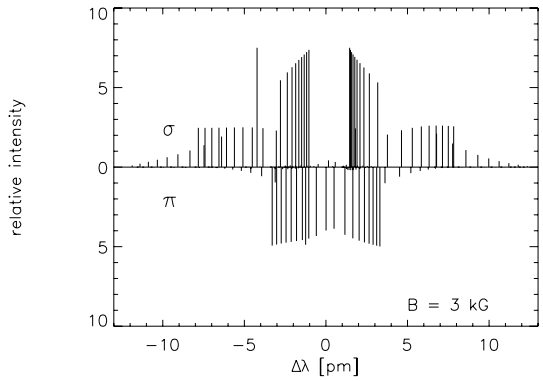

Figure 6. Combined Zeeman and hyperfine splitting of the In I 451.13-nm line in a magnetic field of 3 kG.

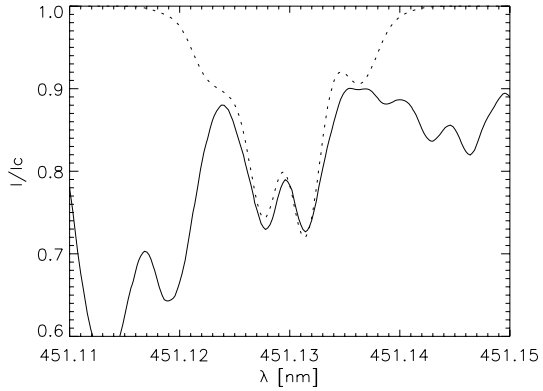

Figure 7. Profiles of the In I 451.13-nm line in the sunspot spectrum. Solid line: Kitt Peak sunspot atlas with 60 per cent straylight subtraction. Dotted line: computed profile with instrumental broadening corresponding to the Kitt Peak FTS (Gaussian with FWHM = 0.47 pm).

but the assumptions made to obtain it are not justified. We conclude that the solar line at this wavelength in the quiet-Sun spectrum is probably not due to indium.

Umbral profile synthesis. We use the appearance of the 451.13-nm line in the sunspot spectrum to provide an independent estimate. In order to include Zeeman splitting, we estimate the magnetic field to be 3000 G from the Ti I 464.52-nm line observed at the same day as the In I 451.13 nm in the Kitt Peak Sunspot atlas. Lines with hyperfine structure split in complex manner in the presence of magnetic fields (Landi degl'Innocenti 1975). We employed the code by Landi degl'Innocenti (1978). The result is shown in Fig. 6. We assume that the orientation of the magnetic field in the observed sunspot is purely vertical and maintains only the σ components.

For the model atmosphere, we use the semi-empirical umbral model M of Maltby et al. (1986). Fig. 7 compares the synthesized profile assuming the meteoritic abundance value $A_{\rm In}^{\rm m} = 0.80$ to the observed profile assuming 60 per cent straylight. The dotted curve is the computed profile after convolution with instrumental broadening corresponding to the FTS resolution of one million. No ad hoc wavelength shift is applied. The match is quite satisfactory including the separation and amplitude ratio of the two peaks.

Obviously, the good match in Fig. 7 requires 60 per cent straylight subtraction. We first argue and then show that this is a reasonable value. In their introduction to the Kitt Peak sunspot atlas, Wallace et al. (2000) already remark that photospheric straylight fully dominates the violet part of the spectrum. Its contribution scales as λ^{-2} (see Staveland 1970) so that it is still large in the blue around 450 nm. Berdyugina, Solanki & Frutiger (2003) used 25 per cent to fit their TiO lines at 705 nm which translates into 61 per cent at 450 nm with the λ^{-2} dependence. In order to quantify this estimate more precisely, we have performed spectral synthesis of the Fe II 436.9-nm line chosen because it is the closest Fe II line without Zeeman splitting to the In I 451.13-nm line. The oscillator strength of the line was adapted to obtain a good fit to the photospheric spectrum as shown in Fig. 8. The lower curves demonstrate that the Fe II line vanishes in the intrinsic umbral spectrum and only appears due to the contribution by photospheric stray light. The good fit to the atlas spectrum was obtained with 65 per cent addition of the computed photospheric spectrum. The reason why the Fe II line vanishes in the umbral spectrum is shown in Fig. 9. The dominant ionization stage is Fe II in the photosphere, but Fe I throughout the low umbral photosphere. Fe II lines that are weak in the photospheric spectrum can therefore not appear in the intrinsic umbral spectrum.

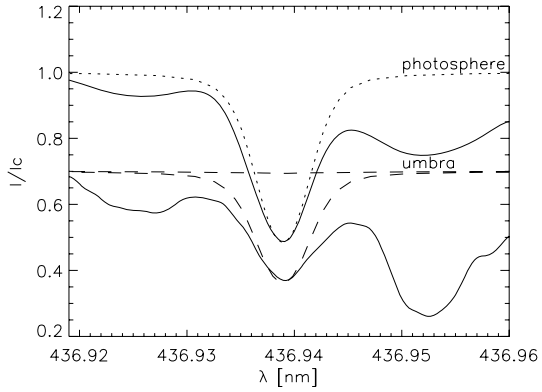

Figure 8. Profiles of the Fe II 436.9-nm line in quiet Sun (upper pair) and umbral spectra (lower curves). The latter are shifted down over 0.3 of the relative intensity scale. Solid line: observed profiles from the Kitt Peak photosphere and sunspot atlases. Dotted line: computed profile from the HOLMUL model. Dashed line: computed profiles using the Maltby M model without and with 65 per cent photospheric straylight addition.

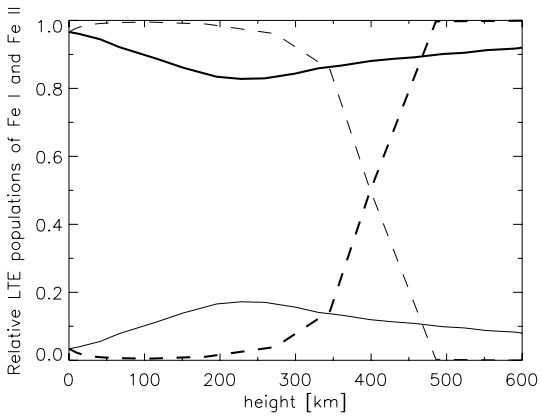

Figure 9. The relative LTE populations of neutral (thin curves) and once-ionized iron (thick curves) in the HOLMUL photosphere model (solid curves) and the Maltby M umbral model (dashed curves).

3 DISCUSSION

Our update in Section 2.1 of the analysis of Allen (1978) did not change the conclusion that there is no combination of

nucleosynthetic processes that can produce a Sn/In ratio as obtained using the most recent solar values, while the chondritic ratio can be easily accounted for. This is a strong indication that the solar abundance of indium cannot be much higher than the meteoritic value. This is also suggested by the absence of the In II resonance line at 158.6 nm.

Furthermore, Fig. 4 shows that standard line synthesis including hyperfine structure does not fit the observed profile for either the high or the low abundance value. In contrast, its appearance in the sunspot spectrum is well reproduced, including hyperfine Zeeman splitting, using the low-meteoritic abundance value (Fig. 7) and assuming a reasonable straylight fraction (60 per cent) and umbral field strength of 3000 G.

These results together suggest that the line at 451.13 nm in the quiet-Sun spectrum is not due to indium but to some other species. It should be from an ion with low ionization energy of the neutral stage since the line disappears in the sunspot spectrum (cf. Fig. 9). The observation by Gonzalez (2006a) of significant trends of the assigned indium abundance with $T_{\rm eff}$ and [Fe/H] in a sample of stars cooler than the Sun suggests that the unidentified transition should have high excitation energy. The best possible candidate in the list of Gonzalez (2006a) would be the Sm II line, but as noted in Section 2.2 this is actually a resonance transition of Sm I.

Finally, an alternative explanation of the In I 451.13-nm line formation might be the effect of departure from local thermodynamical equilibrium. In particular, the appearance of the 451.13-nm line as emission line in the spectra of long-period variables during the downward modulation phase was explained already by Thackeray (1937) as optical pumping between Hδ and a In I line at 410.1 nm which shares its upper level with In I 451.13 nm. However, this mechanism does not operate at all in the deep solar photosphere where the formation of the hydrogen Balmer lines is close to LTE (cf. fig. 30 of Vernazza, Avrett & Loeser 1981).

In conclusion, we suggest that the solar indium abundance is close to the meteoritic value as evidenced in the sunspot spectrum, whereas the feature at 451.13 nm in the quiet-Sun spectrum remains unidentified and is likely to be an ion line at high excitation energy from a species with low-first ionization energy.

ACKNOWLEDGMENTS

We are indebted to Stevan Djeniže for drawing our attention to the solar indium abundance, and to Pit Sütterlin and Karl-Ludwig Kratz for discussions. We thank the referee for suggesting the analysis in Fig. 8. This research project has been supported by a Marie Curie Early Stage Research Training Fellowship of the European Community's Sixth Framework Programme under contract number MEST-CT-2005-020395. ML is supported by NWO (VENI fellow). The Ministry of Science of Serbia partially supported this research (project 'Stellar and Solar Physics', Contract No. 146003).

REFERENCES

Allen M. S., 1978, ApJ, 219, 307
Arlandini C., Käppeler F., Wisshak K., Gallino R., Lugaro M., Busso M., Straniero O., 1999, ApJ, 525, 886
Asplund M., Grevesse N., Sauval A. J., 2005, in Barnes T. G. III, Bash F. N., eds, ASP Conf. Ser. Vol. 336, Cosmic Abundances as Records of Stellar Evolution and Nucleosynthesis. Astron. Soc. Pac., San Francisco, p. 25
Berdyugina S. V., Solanki S. K., Frutiger C., 2003, A&A, 412, 513
Bord D. J., Cowley C. R., 2002, Sol. Phys., 211, 3
Carlsson M., 1992, in Giampapa M. S., Bookbinder J. A., eds, ASP Conf. Ser. Vol. 26, Cool Stars, Stellar Systems and the Sun. Astron. Soc. Pac., San Francisco, p. 499
Corliss C. H., Bozman W. R., 1962, Experimental Transition Probabilities for Spectral Lines of Seventy Elements. NBS Monograph, US Department of Commerce, National Bureau of Standards, Washington
Curdt W., Brekke P., Feldman U., Wilhelm K., Dwivedi B. N., Schühle U., Lemaire P., 2001, A&A, 375, 591
Delbouille L., Roland G., Neven L., 1973, Atlas photométrique du spectre solaire de λ 3000 Å, à λ 10000 Å. Institut d'Astrophysique, Université de Liège, Liège
Farouqi K., 2005. PhD thesis, Univ. Mainz, Germany
Fuhr J. R., Wiese W. L., 2006, in Lide D. R., ed., CRC Handbook of Chemistry and Physics, 87th edn. CRC Press, Inc., Boca Raton, FL
Goldberg L., Muller E. A., Aller L. H., 1960, ApJS, 5, 1
Gonzalez G., 2006a, MNRAS, 371, 781
Gonzalez G., 2006b, MNRAS, 370, L90
Grevesse N., Sauval A. J., 1998, Space Sci. Rev., 85, 161
Gurtovenko E. A., Kostyk R. I., 1989, Fraungoferov Spektr i Sistema Solnechnykh Sil Ostsilliatorov. Nauk. Dumka, Kyiv
Holweger H., Müller E. A., 1974, Sol. Phys., 39, 19
Jackson D. A., 1981, Physica, 103C, 437
Kratz K.-L., Farouqi K., Pfeiffer B., Truran J. W., Sneden C., Cowan J. J., 2007, ApJ, 662, 39
Kupka F., Piskunov N., Ryabchikova T. A., Stempels H. C., Weiss W. W., 1999, A&AS, 138, 119
Kurucz R., Bell B., 1995, Atomic Line Data (Kurucz CD-ROM 23). Smithsonian Astrophysical Observatory, Cambridge, MA
Lambert D. L., Mallia E. A., Warner B., 1969, MNRAS, 142, 71
Landi degl'Innocenti E., 1975, A&A, 45, 269
Landi degl'Innocenti E., 1978, A&AS, 33, 157
Lodders K., 2003, ApJ, 591, 1220
Maltby P., Avrett E. H., Carlsson M., Kjeldseth-Moe O., Kurucz R. L., Loeser R., 1986, ApJ, 306, 284
Meyer B. S., 1994, ARA&A, 32, 153
Morton D. C., 2000, ApJS, 130, 403
Rutten R. J., 2002, J. Astron. Data, 8, 8
Simmerer J., Sneden C., Cowan J. J., Collier J., Woolf V. M., Lawler J. E., 2004, ApJ, 617, 1091
Sobelman I. I., 1992, Atomic Spectra and Radiative Transitions. Springer, Berlin
Staveland L., 1970, Sol. Phys., 12, 328
Thackeray A. D., 1937, ApJ, 86, 499
Travaglio C., Gallino R., Arnone E., Cowan J., Jordan F., Sneden C., 2004, ApJ, 601, 864
Vernazza J. E., Avrett E. H., Loeser R., 1981, ApJS, 45, 635
Wallace L., Hinkle K., Livingston W., 1998, An Atlas of the Spectrum of the Solar Photosphere from 13500 to 28000 cm^{-1} (3570 to 7405 Å). NOAO, Tucson, AZ
Wallace L., Hinkle K., Livingston W., 2000, An Atlas of Sunspot Umbral Spectra in the Visible, from 15000 to 25500 cm^{-1} (3920 to 6664 Å). NOAO, Tucson, AZ
Zaal G. J., Hogervorst W., Elie E. R., Bouma J., Blok J., 1978, J. Phys. B: At. Mol. Opt. Phys., 11, 2821
Zwaan C., 1965, PhD thesis, Univ. Utrecht, The Netherlands

This paper has been typeset from a TEX/LATEX file prepared by the author.